Journal of Hazardous Materials 387 (2020) 121672

Contents lists available at ScienceDirect

Journal of Hazardous Materials

journal homepage: www.elsevier.com/locate/jhazmat

Electrochemical determination of nitroaromatic explosives at boron-doped diamond/graphene nanowall electrodes: 2,4,6-trinitrotoluene and 2,4,6-trinitroanisole in liquid effluents

A. Dettlaff[a,*], P. Jakóbczyk[a], M. Ficek[a], B. Wilk[b], M. Szala[c], J. Wojtas[c], T. Ossowski[d], R. Bogdanowicz[a]

[a] Gdańsk University of Technology, Faculty of Electronics, Telecommunications and Informatics, Narutowicza 11/12, 80-233, Gdańsk, Poland
[b] Gdańsk University of Technology, Faculty of Civil and Environmental Engineering, Narutowicza 11/12, 80-233, Gdańsk, Poland
[c] Military University of Technology, S. Kaliskiego 2, 00-908, Warsaw, Poland
[d] University of Gdańsk, Faculty of Chemistry, Bażyńskiego 8, 80-309, Gdańsk, Poland

GRAPHICAL ABSTRACT

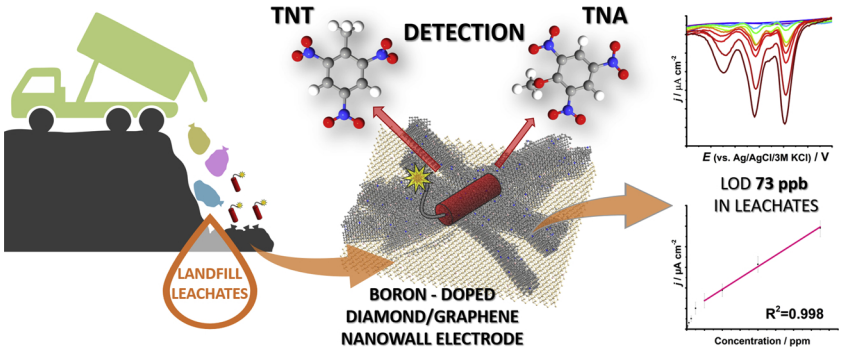

ARTICLE INFO

Editor: Danmeng Shuai

Keywords:
Trace explosives determination
Carbon nanowalls
TNT
Landfill leachates
DPV

ABSTRACT

The study is devoted to the electrochemical detection of trace explosives on boron-doped diamond/graphene nanowall electrodes (B:DGNW). The electrodes were fabricated in a one-step growth process using chemical vapour deposition without any additional modifications. The electrochemical investigations were focused on the determination of the important nitroaromatic explosive compounds, 2,4,6-trinitrotoluene (TNT) and 2,4,6-trinitroanisole (TNA).

The distinct reduction peaks of both studied compounds were observed regardless of the pH value of the solution. The reduction peak currents were linearly related to the concentration of TNT and TNA in the range from 0.05–15 ppm. Nevertheless, two various linear trends were observed, attributed respectively to the adsorption processes at low concentrations up to the diffusional character of detection for larger contamination levels. The limit of detection of TNT and TNA is equal to 73 ppb and 270 ppb, respectively. Moreover, the proposed detection strategy has been applied under real conditions with a significant concentration of interfering compounds – in landfill leachates.

The proposed bare B:DGNW electrodes were revealed to have a high electroactive area towards the voltammetric determination of various nitroaromatic compounds with a high rate of repeatability, thus appearing to be an attractive nanocarbon surface for further applications.

* Corresponding author.
E-mail address: anna.dettlaff@pg.edu.pl (A. Dettlaff).

https://doi.org/10.1016/j.jhazmat.2019.121672
Received 20 July 2019; Received in revised form 9 November 2019; Accepted 11 November 2019
Available online 11 November 2019

1. Introduction

2,4,6-trinitrotoluene (TNT) and 2,4,6-trinitroanisole (TNA, 1-methoxy-2,4,6-trinitrobenzene) belong to secondary explosives, which are commonly used by the military. They are used as the main charge for boosting explosives. TNT and TNA are designed to detonate only under specific conditions and require a detonator or a supplementary booster. 2,4,6-trinitrotoluene (Fig. S1a) is characterised by extremely rapid decomposition and pressurisation (Singh, 2007). 2,4,6-trinitroanisole is a well-known representative of the polynitroderivatives of alkoxybenzene (Fig. S1b); it is one of the safest, most insensitive of HEMs (high energy materials). The energetic properties of TNA are higher than TNT's due to the more positive oxygen balance (Šarlauskas, 2010). Both compounds have relatively low melting points (80.1 and 68.4 °C for TNT and TNA, respectively) and are classified as melt-cast explosives.

Chemical pollution of soil and water, caused by TNT and TNA, is present in places where munitions were previously produced, loaded, or stored. Additionally, in the environment of these explosives, there are also compounds such as nitroso, hydroxylamine, and aniline intermediates that may be highly toxic and recalcitrant. The derivatives of polynitroaromatics were formed by a partial reduction in the aerobic conditions. In mammals, some of these compounds can cause changes in DNA, which may influence their mutagenesis and carcinogenesis (Hundal et al., 1997). The effect of exposure to these explosives on humans is blood disorders, such as anaemia, and abnormal liver function. Nitroaromatics are also noxious to rats, mice, fish, and marine life, and inhibit the growth of many fungi, yeasts, actinomycetes, and gram-positive bacteria (Spiker et al., 1992). TNT and TNA have been claimed to be toxic to humans above 2.0 ppm, and the lifetime health advisory limit has been set at 2 ppb in drinking water (Singh, 2007; A. for T.S. and Registry, 1995; Protection et al., 2017; Gaurav and Malik, 2009). Furthermore, it is dangerous that TNT and TNA are able to penetrate the skin rapidly. They can spawn the formation of methaemoglobin on acute dermal exposure and anaemia on long-term contact.

There are requirements for detection devices used to detect and prevent hazards related to the occurrence of explosive aromatic compounds. The ideal devices should be small, portable, and able to sense trace amounts of explosives with high precision, quickly, and without significant cost (Singh, 2007). The presence of TNT and TNA can be identified by many methods, for example high performance liquid chromatography (Wu et al., 1999), chromatography with UV absorption (Harvey and Clauss, 1996; Babaee and Beiraghi, 2010), electrochemistry (Sekhar et al., 2011; O'Mahony and Wang, 2013a; Pon Saravanan et al., 2006), ion mobility spectrometry (Furton et al., 2015), mass spectroscopy (Lee et al., 1934), chemiluminescent detection (Pittman et al., 2009), electro-kinetic capillary electrophoresis (Oehrle, 2003), fluorescence (Tu et al., 2008), enhanced Raman scattering (Jamil et al., 2015), infrared spectroscopy (Stahl and Tilotta, 2001; López-López and García-Ruiz, 2014), nuclear quadrupole resonance (Grechishkin and Sinyavskii, 2008; Mozjoukhine, 2000), surface plasmon resonance spectroscopy (Shankaran et al., 2005; Riskin et al., 2009), and immunochemistry (Narang et al., 1997; Zeichner et al., 2002). The sensitivity of these methods ranges from 0.06–5000 ppb. Almost all of the techniques require very complicated and expensive instruments which are often nonmobile and not sensitive enough to detect trace amounts of nitroaromatic compounds. Moreover, the reported methods demand the determination be performed in special laboratories by highly qualified staff (Pittman et al., 2009). On the other hand, immunological sensors have been developed that meet almost all of these requirements. The basis of all immunosensors is the specific binding of antigens to antibodies to form a stable immune complex. Although immunosensors are known for their selectivity, they cannot be used in many places because they use antibodies as the detection device, and these reacted antibodies are not reusable (Narang et al., 1997; Zeichner et al., 2002; Bart et al., 1997; Rabbany et al., 2000).

Electrochemical sensors seem to be a promising solution in nitroaromatic detection due to their low cost, portability, and high sensitivity. These devices provide information about the system composition in real-time by combining a chemically selective layer with an electrochemical transducer. Thereby, the chemical energy of the specific interaction between the chemical substances and the sensor is converted into an analytically useful signal. The presence of nitro groups in TNA and TNT with redox properties makes electrochemical methods ideal for their detection. We can distinguish several electrochemical methods depending on: a change of current for an electrochemical reaction with an applied voltage, and with time (voltammetric and amperometric respectively), a change of conductivity (conductometric), a change of membrane potential (potentiometric), and a change of impedance (impedimetric) (Singh, 2007; O'Mahony and Wang, 2013b).

Dynamic methods are becoming exceptionally attractive among electrochemical methods due to their high sensitivity and simplicity in data acquisition. Small and relatively inexpensive portable potentiostats are now available for field applications, but they still require advancement in their sensitivity and lifespan. Carbon materials also are a development direction of electrochemical sensors for the detection of explosives. In the literature, many authors are focussing their attention on the modification of carbon layers (*e.g.*, functionalised nanotubes, graphene) with metallic nanoparticles, such as gold (Roddey and Development, 2011; Zhang et al., 2015a; Schnorr et al., 2013; Avaz et al., 2017; Yew et al., 2016; Akhgari et al., 2015; Yu et al., 2017; Zhang et al., 2006a).

Many electrochemical methods have been reported for the sensing of TNT with a good limit of detection, including nitrogen and sulphur co-doped graphene nanoribbons (LOD: 0.1 ppb) (Zhang et al., 2018a), carbon nanotubes (Roddey and Development, 2011; Zhang et al., 2006a), oligomer-coated carbon nanotubes (LOD: 95 ppb) (Zhang et al., 2015a), glassy carbon electrodes modified with multi-wall carbon nanotubes (LOD: 0.6 ppb) (Wang et al., 2004) and their modifications. There is only one paper about the detection of TNT on boron-doped diamond (de Sanoit et al., 2009). However, the preparation of the electrodes is a multistep process including chemical and electrochemical oxidation of the electrode.

In this article, we propose a novel sensor based on a boron-doped diamond/graphene nanowall electrode prepared by a one-step chemical vapour deposition process. The detection was conducted using a dynamic electrochemical technique (differential pulse voltammetry), and the explosives were determined in aqueous solutions, including liquid effluents. To the authors' knowledge, this is the first time diamond/graphene nanowall electrodes have been shown to detect nitroaromatic explosives.

A boron-doped diamond/graphene nanowall electrode is a hybrid electrode, which combines the extraordinary features of boron-doped diamond and a graphene nanowall on the same surface. B:DGNW is an sp^2-rich phase material (Yu et al., 2011; Sobaszek et al., 2017) with multilayered graphene walls oriented vertically to the substrate. The high sensitivity of a boron-doped diamond/graphene nanowall electrode is attributed to the fact that TNT and TNA are good *p*-electron acceptors and easily adsorb onto the *p*-electron-rich graphene surface *via* π-π electron donor-acceptor (EDA) stacking interactions (Zhang et al., 2018b). The presence of the boron-doped diamond phase enhances the electrochemical performance and kinetics of the electrode surface when compared with typical carbon nanowalls. The main advantage of a B:DGNW electrode is the developed active surface which is about three times higher than a boron-doped diamond electrode. The material can be considered to be a 3D-structure nanomaterial.

The electrochemical sensing platform fabricated from diamond/graphene nanowall electrodes showed a sensitive and selective response to nitroaromatic type energetic materials with a detection limit of 73 ppb and 270 ppb for TNT and TNA, respectively. The use of a

B:DGNW electrode leads to a strong interfacial accumulation of 2,4,6-trinitrotoluene and 2,4,6-trinitroanisole, and hence offers a determination of these compounds in an extremely complicated, real matrix such as landfill leachates, with satisfactory results.

2. Experimental

2.1. Chemicals

TNT was purchased from Nitro-Chem JSC (Poland), TNA was synthesised in the Military University of Technology according to an original, unpublished procedure based on known a method (Spencer and Wright, 1946) and recrystallised two times from ethanol. All reagents were analytical grade and used without further purification. HPLC-grade extra pure acetonitrile was used to prepare the 2,4,6-trinitrotoluene and 2,4,6-trinitroanisole stock solutions.

2.2. Preparation of solutions

Due to the low solubility of 2,4,6-trinitrotoluene and 2,4,6-trinitroanisole in water (for TNT 100 mg L^{-1} at 25 °C (Ro et al., 1996)), standard stock solutions of individual explosives at 1000, 100, 10, 1 ppm concentrations were prepared in acetonitrile. For the cyclic voltammetry (CV) and differential pulse voltammetry (DPV) tests, with different TNT and TNA concentrations for analysis, the aliquot volume of the standard stock solutions was added to 10 mL of electrolyte. The DPV tests were performed in 1 mL of sample solution consisting of 0, 0.01, 0.05, 0.1, 0.25, 0.5, 1.0, 2.0, 4.0, 8.0 and 16 ppm of TNT or TNA in 0.5 M KCl and 0.1 M phosphate buffered saline (PBS), pH = 6.7. The KCl solution was used due to the high amount of chlorides inside the tested real-life sample - landfill leachates (see Table S1), whereas the PBS buffer enables the pH value to be precisely controlled. For the CV tests 20 ppm of TNT and TNA in phosphate buffer electrolyte with KCl at different pH levels of 5.6, 6.7 and 8.0 were made, and also 20 ppm of TNT and TNA in landfill leachate and with 0.5 M KCl.

2.3. Electrode growth

The B:DGNW electrodes were synthesised using a microwave plasma enhanced chemical vapour deposition system (SEKI Technotron AX5400S, Japan). The detailed parameters of the thin film synthesis for the B:DGNW can be found in (Sankaran et al. (2018)) and (Siuzdak et al. (2017a)). All samples were doped by using diborane (B_2H_6) as an acceptor precursor. The [B]/[C] ratios in the plasma were set to 2k ppm, which resulted in the boron being incorporated into the multi-layered diamond/graphene nanowall layer (Sobaszek et al., 2017). An external heater was used to heat the substrate to a temperature of about 700 °C, while the substrate temperature was measured using a thermocouple embedded in the substrate holder. Several B:DGNW samples were fabricated. The growth time was 6 h. The B:DGNW thin films were grown on (100) oriented silicon substrates. Prior to CVD growth, the Si substrates were seeded by spin-coating in a diamond slurry (Ficek et al., 2015). X-ray photoelectron spectroscopy (XPS) measurements were carried out to more clearly reveal the surface chemical bonding characteristics of the boron-doped diamond/graphene nanowall which was presented before (Siuzdak et al., 2017b). The morphology and molecular composition of B:DGNW was presented in (Sankaran et al. (2018)).

2.4. Characterisation techniques

The electrochemical studies were carried out using the differential pulse voltammetry (DPV) and cyclic voltammetry (CV) techniques. The measurements were made with a potentiostat–galvanostat (VMP-300, Bio-Logic, France) *via* the EC-Lab software. All electrochemical tests were conducted in a three-electrode electrochemical cell in an argon atmosphere at room temperature (22 ± 1 °C). The boron-doped diamond/graphene nanowall electrodes were used as the working electrodes, an Ag/AgCl/3.0 M KCl electrode served as the reference electrode, whereas a Pt wire served as the counter electrode. The geometric area of the working electrode was around 0.20 cm^2.

Differential pulse voltammograms were obtained under the following conditions: the potential ranging from −0.15 to −0.7 V (*vs.* Ag/AgCl/3.0 M KCl), a 200 ms pulse width, a 25 mV pulse height, a step time of 500 ms, and a scan rate of 10 mV s^{-1}.

The CV measurements were conducted in 0.5 M KCl containing solution 0.1 M PBS (pH = 6.7), and measured for chosen sweep rates in the 10 − 300 mV s^{-1} range. The potential range was from -0.8 V to 0.5 V *vs.* Ag/AgCl/3.0 M KCl. Furthermore, cyclic voltammetry was performed in 0.5 M KCl and 0.1 M PBS solution at pH 5.6, 6.7, and 8.0 in the range -1.0 to 0.5 V. Likewise, cyclic voltammetry was used for the determination of 20 ppm TNT and TNA in 1 mL of landfill leachate and landfill leachate with KCl added, c = 0.5 moL dm^{-3} (ν = 100 mV s^{-1}; E = −1.0 V – 0.5 V).

2.5. Landfill leachate

To prove the potential of the proposed electrochemical sensor, the measurements were also performed in a real-life sample, in landfill leachate. For this purpose, three leachate samples were collected for this experiment in December 2018 from the 'Eko Dolina Łężyce' municipal solid waste plant, situated in northern Poland. Wastewater samples were taken in high-density polyethylene (HDPE) bottles at the bottom of a cell from an unaerated storage reservoir. The cooled leachate (4 °C) was transported (in a portable refrigerator) to the laboratory, then homogenised and kept frozen (−20 °C) until the analyses took place. The main characteristics of the leachate were: a pH in the alkaline range (7.8 ± 0.1), a dark brown colour (see Fig. S2), total nitrogen (2263.3 ± 56.9 mg N L^{-1}), total carbon (2142.7 ± 138.5 mg C L^{-1}), total phosphorus (16.2 ± 0.6 mg TP L^{-1}), high concentrations of ammonium nitrogen (96.0 % ± 2.8 % of the total nitrogen) and chemical oxygen demand (3893.3 ± 21.6 mg O_2 L^{-1}), the phosphorus occurred mainly as P-PO_4 (69.2 % ± 5.8 % of the total phosphorus), a low BOD_5/COD ratio (0.07 ± 0.005), and high concentrations of chloride and sulfate (with mean values 2609.8 ± 87.7 mg Cl^- L^{-1} and 1650.0 ± 115.2 mg SO_4^{2-} L^{-1}, respectively). The detailed characteristics of the raw landfill leachate are listed in Table S1.

3. Results and discussion

The electrochemical behaviour largely depends on the features of the working electrode material. Due to its remarkable physical and electrochemical properties, B:DGNW has attracted much attention for the development of high-performance electrochemical sensors. The B:DGNW electrode is characterised by a wide electrochemical potential window and low background currents regardless of the pH of the solution (Fig. S3a). The widest potential window, equal to 2.85 V, was obtained for the KCl salt. The B:DGNW electrodes also show a low peak-to-peak separation value recorded for the ferricyanide/ferrocyanide redox system (61 mV for ν = 5 mV s^{-1}), which confirms the rapid electron transfer (Fig. S3b). It should be noted that, unlike the boron-doped diamond electrodes, the B:DGNW electrodes are not characterised by a shift in oxygen reduction potential towards more negative potentials. The reduction signal for the B:DGNW electrode occurs at −0.31 V (Fig. S4). Therefore, deoxidation of the electrolyte prior to electrochemical measurements is a necessary step.

The detection of the explosives was first established in 0.5 M KCl containing 0.1 M standard phosphate buffer by using cyclic voltammetry in the acidic (pH = 5.6), neutral (pH = 6.7) and basic electrolytes (pH = 8.0) (see Fig. 1).

Cyclic voltammograms of TNT revealed three distinct reduction peaks regardless of the solutions' pH values. The peaks are labelled 1.,

2., and 3. by order of appearance in the CV cathodic wave (Fig. 1a). The reduction of polynitroaromatic compounds proceeds by multistep processes. Each of the peaks reflects the individual reduction of an acceptor -NO_2 group according to the mechanism showed in Fig. 2a (Yew et al., 2016; Zhang et al., 2018b; Chua et al., 2012; Chua and Pumera, 2011; Bratin et al., 1981; Wang, 2007). The most probable path of the TNT reduction mechanism starts with the *ortho*-NO_2 group reduction (E_{red1}). Subsequently, the reduction of the second nitro moiety in *ortho*-position takes place (E_{red2}). The last, 3. peak, probably corresponds to the reduction of the third *para*-nitro group (Chua et al., 2012). Consequently, each -NO_2 group undergoes 6-electron reduction to a -NH_2 moiety. Overall, the electrochemical reduction of trinitroaromatic explosives consumes 18 electrons and 18 protons coming from the solvent. As a result 2,4,6-triaminotoluene is formed.

The reduction process begins by the transfer of 1e- and $1H^+$ originating from the electrolyte (Fig. 2b). As a result, a neutral radical is created (TNT-$H^{\cdot}$). Along with the next transfer of 1e- and $1H^+$, the proton is attached to the oxygen of the intermediate. Subsequently, the water molecule is removed and nitroso intermediate is formed. After other steps, including protonation the hydroxylamine is obtained. Finally, the next 2e-/$2H^+$ reduction leads to the creation of an amine group.

The described reduction process heavily depends on the solvent pH. It is noteworthy that with an increasing pH value, the maxima of the reduction peaks shift to the more negative potentials (see Fig. 1a–b). The detailed values of the peak heights and maxima are shown in Table S2. For instance, the first reduction peak of 2,4,6-trinitrotoluene recorded in the pH range of 4.0–9.0 (see Fig. S5) shifts from −0.3 V to −0.48 V. The same phenomenon was also observed for 2,4-dinitrotoluene and 2,4,6-trinitrotoluene detected on a glassy carbon electrode by Pumera et al. (Chua and Pumera, 2011; Toh et al., 2013). Such a response may be explained by the involvement of hydronium ions in the reduction process of the nitro moieties.

The TNA and TNT compounds were reduced to many radical forms according to the general mechanism presented in Fig. 2. Due to the high reactivity of the radical molecules and the susceptibility to proton reactions and kinetic conditions, in the diffusion layer, the real concentrations of individual reduced forms may differ from the assumed mechanism.

Changing the position of reduction peaks and especially oxidation peaks (reoxidation) as a function of pH shows variability. The height of the reaction peaks with the changing of pH changed. It should be taken into account that the rate of subsequent reactions leading to the formation not only reduced forms and their protonated forms but also nitro-hydroxylamine and amine forms. The complexity of the TNT and TNA reduction mechanism may additionally be associated with different rates of individual reduction step, changes in diffusion coefficients for differently charged intermediates, and others. The combined effect of these factors can determine that the reduction peaks appeared at different magnitudes.

It should be noted that a higher catalytic activity of the B:DGNW electrode was achieved for TNT. Furthermore, the most desirable signal-to-background characteristics were achieved in a 6.7 pH solution for both nitro compounds. The weaker response was for the 5.6 pH solution. In the basic medium, in turn, low-intensity peaks were observed. The best electrochemical performance of the electrode in the acidic environment coincided with other reports (Pon Saravanan et al., 2006; Zhang et al., 2006b, b). Therefore we decided to use a solution with a pH of 6.7 throughout the following electrochemical measurements.

Additionally, the boron-doped diamond electrodes (B:DD), prepared according to (Ryl et al., 2016), were used for comparative studies. The current densities and kinetics of both B:DD and B:DGNW electrodes were illustrated in Fig. S6. The B:DGNW electrode results in much higher current densities *vs.* TNT detection, thus it enables efficient determination with lower LOD when compared with BDD.

The next step was an examination of the scan rate (ν) effect on the reduction peak current of the explosives (Fig. 3). It is noteworthy that as the scan rate value increases, the current signal also increases. The plots shown in Fig. 3c–d present a linear response in the range 10 – 300 mV s^{-1} for both nitro compounds. The cathodic peaks of 2,4,6-trinitrotoluene are more separated than for 2,4,6-trinitroanisole. Moreover, with an increasing scan rate, there is a shift of the reduction peaks' maxima to a more negative potential, which confirms the irreversibility of the nitro compounds' reduction. The maximum peak current densities and reduction potentials are gathered in Table S3. The linear dependence of i_{pc} *versus* $\nu^{0.5}$ suggests the diffusional control of the reduction process.

It can be seen that in 6.7 pH TNA for 100 mV s^{-1}, there are four electrochemical reduction peaks, which is significantly different from TNT. This means that the reduction of nitroaromatic compounds, such as TNA, is a rather complex process and depends not only on the number of nitro groups, but also the presence of other moieties. However, depending on the experimental conditions, 3–4 reduction signals were detected. Each nitro group is reduced to the amine form. The additional peak, localised at 0.4 – 0.5 V (peak 2a.), may correspond to the mechanism mentioned in the literature (Junqueira et al., 2013), in which there is a two-step reducing mechanism to hydroxylamines. The first step is slow: the nitro compound is reduced to a radical anion. In the second step, hydroxylamine is obtained. Different reaction rates can be confirmed by the appearance of additional peaks at the lower scan rates. Also, the presence of a forth peak in pH close to neutral may be associated with the presence of protons in the reaction mechanism and the absence of a second peak for an alkaline medium.

Differential pulse voltammetry was used for quantification purposes. DPV measurements were performed in 6.7 pH in 0.5 M KCl containing 0.1 M PBS (Fig. 4). For TNT, three well-separated peaks were observed at −0.32 V, −0.44 V, and −0.56 V. The voltammograms of

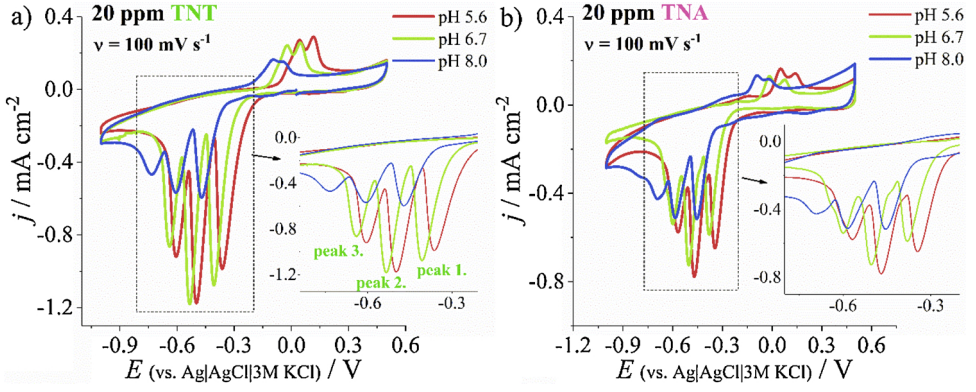

Fig. 1. Current densities of 20 ppm solution of a) TNT, b) TNA recorded on B:DGNW in 0.5 M KCl/0.1 M PBS at different pHs; scan rate 100 mV s^{-1}.

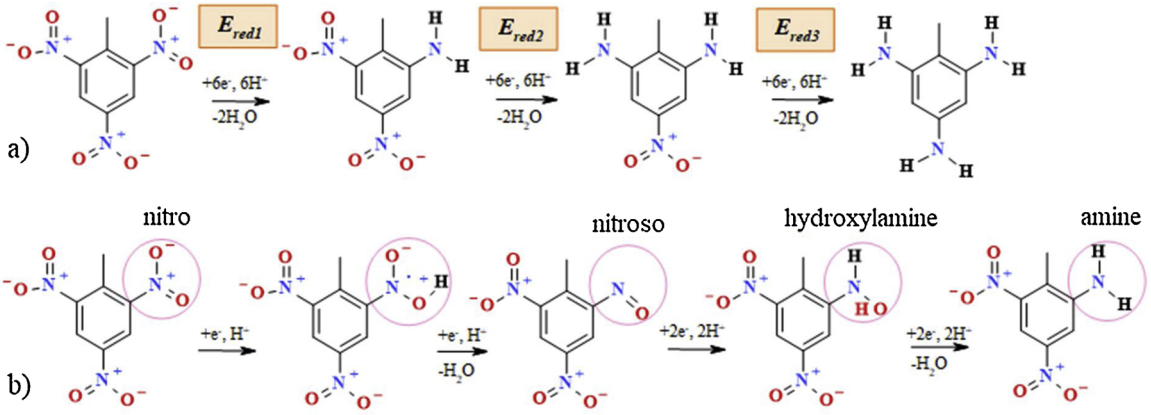

Fig. 2. The mechanism of reduction of a) three nitro groups in the most likely sequence, b) the one nitro moiety (in the ortho position) in an aqueous solution.

the 2,4,6-trinitroanisole response contain four peaks similarly to the aforementioned CV tests: three well-developed at −0.29, −0.42 V, −0.55 V, and one not completely separated at −0.36 V. The first reduction peak observed at about −0.56 V exhibited the most favourable characteristics for TNT and TNA, and was chosen for the subsequent quantitative analysis. Calibration curves (y = ax + b) for the first reduction peak obtained in the 0.5 M KCl with 0.1 M phosphate buffer solution for TNT and TNA are shown in Fig. 4c–d. The dependence of the current density reduction peaks' intensity *vs.* the concentration of both nitro compounds exhibits two different linear responses depending on the concentration of the explosive. The calibration curves were found to be linear within the range of 0.05–2 ppm and 4–15 ppm for 2,4,6-trinitrotoluene (R^2 = 0.999, R^2 = 1.00 respectively, N = 3), and 0.05–1 ppm and 2–15 ppm for 2,4,6-trinitroanisole (R^2 = 0.998, R^2 = 0.998 respectively, N = 3). When the concentration was larger than 2 ppm for TNT or 1 ppm for TNA, the mechanism of detection changed from the adsorption-controlled process to the diffusional one. For electrodes with a nanoporous structure, the process of compound deposition is observed inside and on the porous structure. At low concentrations of analyte, the more accessible active surface area could be completely covered due to low competition for the surface. This phenomenon enables a more efficient uptake of TNT and TNA, leading to a higher sensitivity for concentrations up to about 1 − 2 ppm. As a result, two linear ranges in the slope appeared (Gao et al., 2014). Similar behaviour was observed by other authors working on carbon electrodes with high amount of porous carbon (Siuzdak et al., 2017a; El Bouabi et al., 2016; Muhammad et al., 2016). It should be noted that most explosives detection reports present only results containing low concentrations of nitro compounds (below 5 ppm) (Zhang et al., 2018b; Sağlam et al., 2018; Filanovsky et al., 2007; Wang et al., 2013; Casey and Cliffel, 2015).

The limit of detection was calculated from LOD = $3\sigma_{bl}/a$, where σ denoted the standard deviation of a blank, and "a" is the slope of the calibration curve, whereas the limit of quantitation of LOQ = $10\sigma_{bl}/a$ (Sağlam et al., 2018; Soomro et al., 2016). The limit of detection for TNT was found to be 73 ppb ($3.22 \cdot 10^{-7}$ M), whereas the LOD for TNA

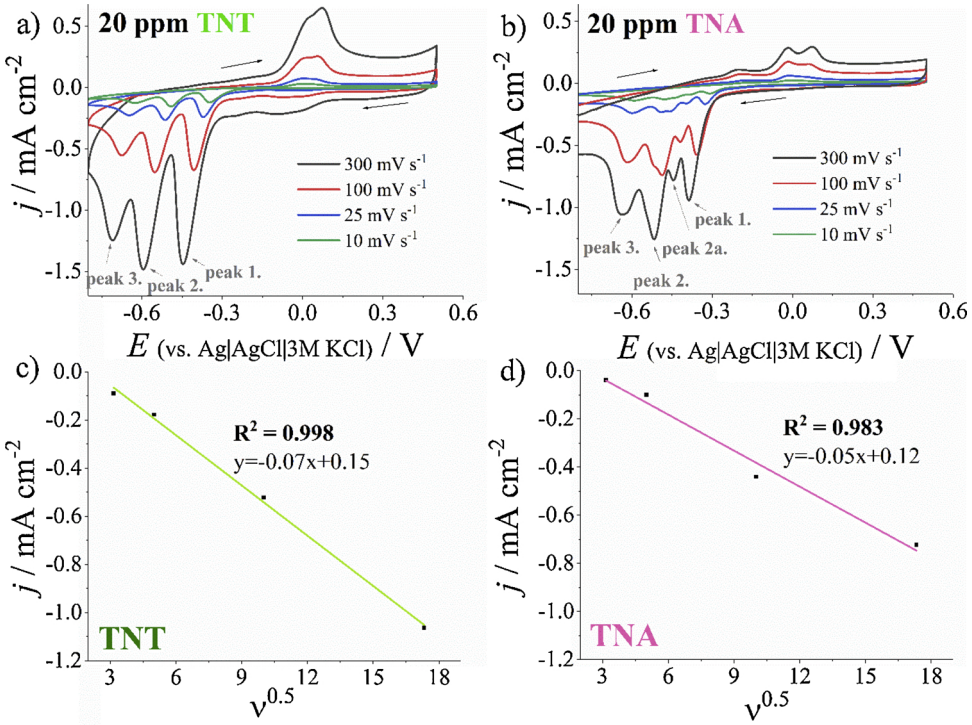

Fig. 3. Cyclic voltammetry recorded as a function of scan rate of 20 ppm solution of a) TNT, b) TNA in 0.5 M KCl + 0.1 PBS on B:DGNW electrode (pH = 6.7). The plot of i_{pc} *versus* $\nu^{0.5}$ for c) TNT, d) TNA for the 1. peak (localised at *ca.* -0.35 V).

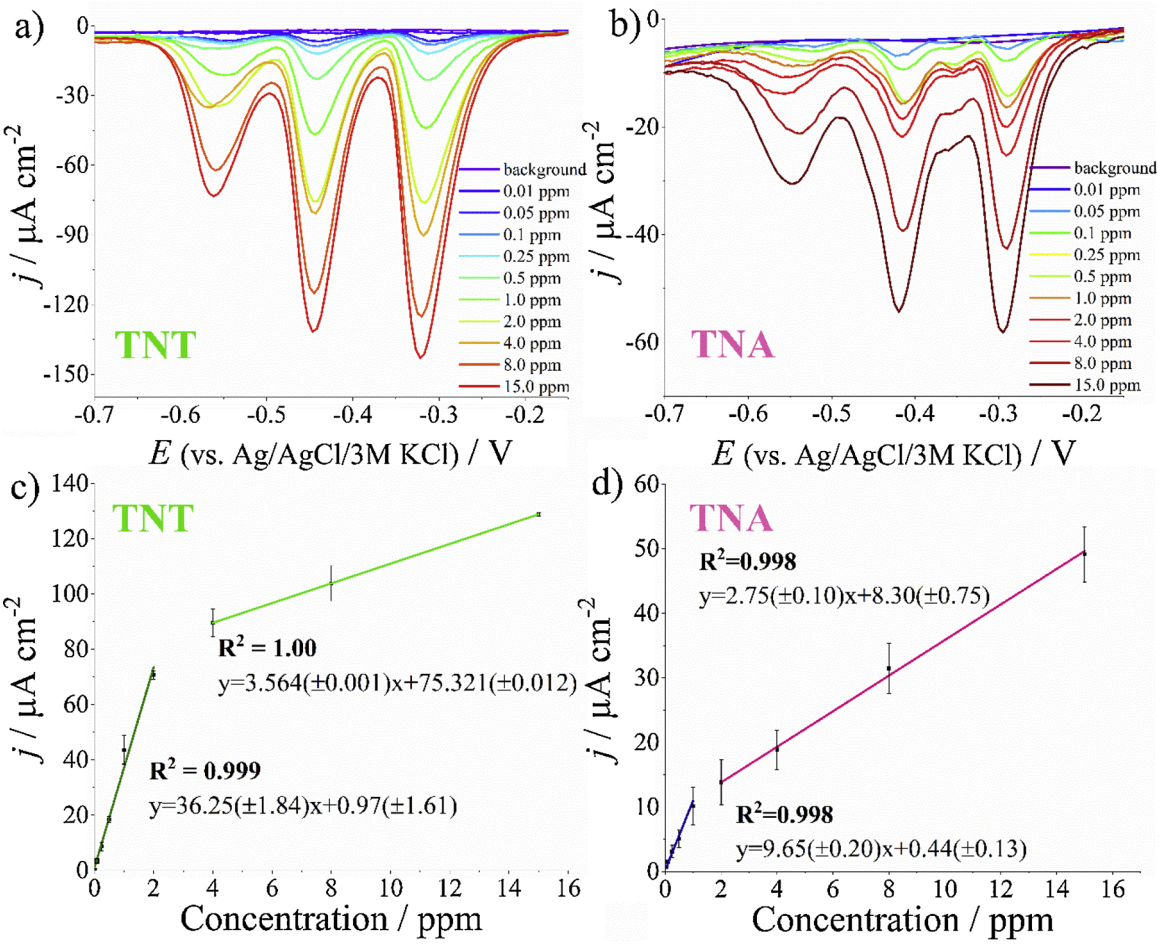

Fig. 4. DPV of a) TNT, b) TNA recorded on B:DGNW; Concentration dependence of c) TNT, d) TNA on B:DGNW based on 1. reduction peak observed at *ca.* -0.3 V (the error bars represent the standard deviation).

Table 1
Comparison of the electroanalytical detection of TNT on different electrodes.

Electrode	LOD / ppb	Linear range / ppm	Ref.
[a]BW-NS-rGONRs	0.1	0.0008 – 5.1	(Zhang et al., 2018b)
Au-graphene	5.9	0.02 – 0.7	(Wang et al., 2013)
[b]GC/P(Cz-co-ANI)-Au_{nano}	25	0.1–1	(Sağlam et al., 2018)
This work	**73**	**0.05 – 2** **4 – 15**	
TiO_2/Pt_{nano}	200	2 – 5	(Filanovsky et al., 2007)
[c]PNEGHN	300	0.5 – 40	(Guo et al., 2010)
Multilayer graphene nanoribbons	1000	1 – 20	(Goh and Pumera, 2011)
Exfoliated graphene	6540	4-20	(Yew et al., 2016)

[a] BW-NS-rGONRs: base washed nitrogen- and sulfur-codoped graphene nanoribbons.

[b] GC/P(Cz-co-ANI)-Au_{nano}: modified glassy carbon electrode coated with poly(carbazole-aniline) copolymer film.

[c] PNEGHN: Pt nanoparticle ensemble-on-graphene hybrid nanosheet.

was 270 ppb ($1.13 \cdot 10^{-6}$ M). The LOQ value was 240 ppb ($1.07 \cdot 10^{-6}$ M) and 940 ppb ($3.77 \cdot 10^{-6}$ M) for TNT and TNA, respectively. The results indicate that B:DGNW exhibits greater electrocatalytic activity towards 2,4,6-trinitrotoluene compared to 2,4,6-trinitroanisole. For instance, the cathodic density current from the first reduction peak for 15 ppm of nitroaromatics is 138 µA cm^{-2} and 52 µA cm^{-2} for TNT and TNA, respectively. The signal recorded for TNT is more than 2.5 times higher. Table 1 shows a comparison of TNT detection performances from the present and previously reported electrochemical methods depending on the electrode used.

The selectivity of the sensing electrode was determined by the measuring of the cathodic peak current of 8 ppm TNT with 0.1 M PBS with different inorganic ions including: 0.5 M Na^+, K^+, SO_4^{2-}, NH_4-, Cl-. The signal change of the reduction current of TNT was less than 5 % in the presence of Na^+, K^+, SO_4^{2-},Cl-. The presence of NH_4- causes an error of 11.5 %. It should be emphasized that TNT reduction is one of the processes generating radicals with a very strong reducing potential. The presence in solution of strong oxidising agents such as oxygen, hydrazine or hydrogen peroxide will cause the fast reaction with the generated TNT radical (for instance TNT-$H^{\cdot}$). Thus, the current signal will be disrupted. In our research, the concentration of interfering factors was significantly lower than the concentration of the basic electrolyte. We did not notice the effect of such factors at a concentration close to the concentration of the analyte being tested.

The reproducibility of the proposed sensor for TNT detection was investigated by determining 8 ppm TNT with six separated electrodes. The results indicate that all of the samples show almost similar responses with a relative standard deviation of 2.8 %. Thus, the electrodes are reproducible.

The stability of the B:DGNW electrode was evaluated by the comparison of the peak-to-peak separation values (ΔE) obtained for the electrode in ferricyanide/ferrocyanide redox before and after 7 days of leaving the electrode in 5 mM $K_3[Fe(CN)_6]$ with 0.5 M Na_2SO_4 solution. The ΔE values gathered in Table S4 confirm good stability of the electrodes.

To prove the potential of the electrochemical detection, the

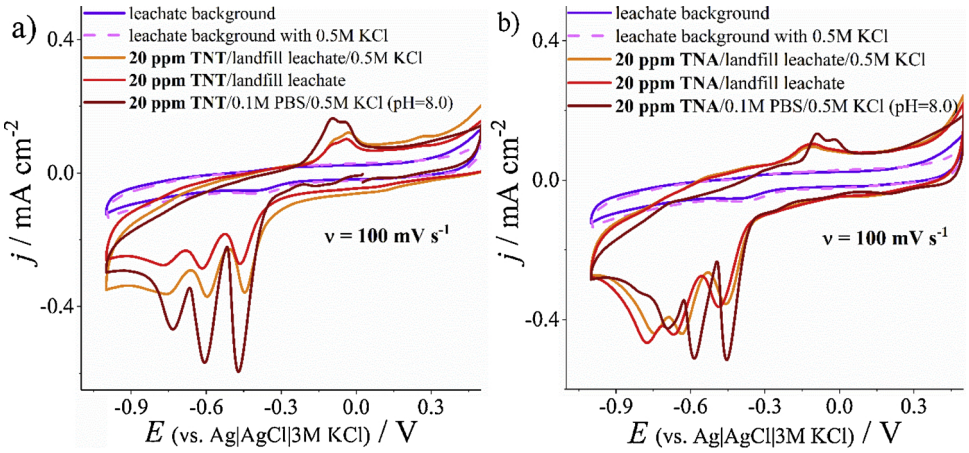

Fig. 5. Determination of a) TNT, b) TNA in landfill leachates and landfill leachates with 0.5 M KCl.

measurements were subsequently performed in a real-life sample, in landfill leachate. The cyclic voltammograms of TNT and TNA determined on a boron-doped diamond/graphene nanowall electrode are presented in Fig. 5. Firstly, CV scans were carried out in a blank electrolyte containing only the leachate (or the leachate with additional 0.5 M KCl) to determine the occurrence of any background interference. In the landfill leachate, TNT, as well as TNA, displayed three reduction peaks on the bare B:DGNW electrode. There was no significant difference in the determination of nitro compounds in landfill leachate and landfill leachate with the addition of KCl, hence, direct detection is possible. In landfill leachate, 2,4,6-trinitrotoluene gives signals at −0.462 V, −0.615 V and −0.768 V. The peak potentials of TNA, in turn, were observed at −0.483 V, −0.665 V, and −0.774 V.

4. Conclusions

In summary, an electrochemical sensing boron-doped diamond/graphene nanowall electrode was used for the detection of two different explosives. Herein, it was shown that a B:DGNW sensor may provide a fast, low-cost, selective and sensitive alternative detection technique of nitroaromatic type energetic materials. Furthermore, a B:DGNW electrode can be successfully applied to 2,4,6-trinitrotoluene and 2,4,6-trinitroanisole detection in landfill leachates. A B:DGNW electrode exhibits high sensing performance for TNT detection with linearity between 0.05–2 ppm and 4–15 ppm, and a detection limit of 73 ppb. The LOD for 2,4,6-trinitroanisole, in turn, is equal to 0.27 ppm. The proposed method is very sensitive and selective even for samples that are highly contaminated. The demonstrated performance has proven that the method has significant application potential and is a very promising tool in the case of the detection of nitroaromatic explosives in liquid effluents. Moreover, the newly described electrode materials can be used in the future to efficiently increase the remediation of waste waters from nitroaromatic synthesis factories.

CRediT authorship contribution statement

A. Dettlaff: Methodology, Validation, Investigation, Formal analysis, Writing - original draft, Visualization. **P. Jakóbczyk:** Methodology, Validation, Investigation, Formal analysis, Writing - original draft. **M. Ficek:** Investigation, Writing - original draft. **B. Wilk:** Resources, Writing - original draft. **M. Szala:** Resources. **J. Wojtas:** Conceptualization, Resources. **T. Ossowski:** Supervision, Writing - review & editing. **R. Bogdanowicz:** Conceptualization, Supervision, Writing - review & editing, Visualization, Project administration, Funding acquisition.

Declaration of Competing Interest

The authors declare that they have no known competing financial interests or personal relationships that could have appeared to influence the work reported in this paper.

Acknowledgements

This work was supported by the Science for Peace Programme of NATO [Grant no. G5147], Polish National Science Centre [2016/22/E/ST7/00102] and the National Centre for Science and Development [347324/12/NCBR/2017]. The DS funds of the Faculty of Electronics, Telecommunications, and Informatics of the Gdansk University of Technology are also acknowledged.

Appendix A. Supplementary data

Supplementary material related to this article can be found, in the online version, at doi:https://doi.org/10.1016/j.jhazmat.2019.121672.

References

A. for T.S, Registry, D., 1995. Toxicological Profile for 2,4,6-Trinitrotoluene. U.S. Dep. Heal. Hum. Serv.https://doi.org/10.1201/9781420061888_ch21.
Akhgari, F., Fattahi, H., Oskoei, Y.M., 2015. Recent Advances in Nanomaterial-Based Sensors for Detection of Trace Nitroaromatic Explosives. Elsevier B.V.https://doi.org/10.1016/j.snb.2015.06.146.
Avaz, S., Roy, R.B., Mokkapati, V.R.S.S., Bozkurt, A., Pandit, S., Mijakovic, I., Menceloglu, Y.Z., 2017. Graphene based nanosensor for aqueous phase detection of nitroaromatics. RSC Adv. 7, 25519–25527. https://doi.org/10.1039/c7ra03860g.
Babaee, S., Beiraghi, A., 2010. Micellar extraction and high performance liquid chromatography-ultra violet determination of some explosives in water samples. Anal. Chim. Acta 662, 9–13. https://doi.org/10.1016/j.aca.2009.12.032.
Bart, J.C., Judd, L.L., Hoffman, K.E., Wilkins, A.M., Kusterbeck, A.W., 1997. Application of a portable immunosensor to detect the explosives TNT and RDX in groundwater samples. Environ. Sci. Technol. 31, 1505–1511. https://doi.org/10.1021/es960777l.
Bratin, K., Kissinger, P.T., Briner, R.C., Bruntlett, C.S., 1981. Determination of nitro aromatic, nitramine, and nitrate ester explosive compounds in explosive mixtures and gunshot residue by liquid chromatography and reductive electrochemical detection. Anal. Chim. Acta 130, 295–311. https://doi.org/10.1016/S0003-2670(01)93007-7.
Casey, M.C., Cliffel, D.E., 2015. Surface adsorption and electrochemical reduction of 2,4,6-trinitrotoluene on vanadium dioxide. Anal. Chem. 87, 334–337. https://doi.org/10.1021/ac503753g.
Chua, C.K., Pumera, M., 2011. Influence of methyl substituent position on redox properties of nitroaromatics related to 2,4,6-trinitrotoluene. Electroanalysis 23, 2350–2356. https://doi.org/10.1002/elan.201100359.
Chua, C.K., Pumera, M., Rulíšek, L., 2012. Reduction pathways of 2,4,6-trinitrotoluene: an electrochemical and theoretical study. J. Phys. Chem. C 116, 4243–4251. https://doi.org/10.1021/jp209631x.
de Sanoit, J., Vanhove, E., Mailley, P., Bergonzo, P., 2009. Electrochemical diamond sensors for TNT detection in water. Electrochim. Acta 54, 5688–5693. https://doi.org/10.1016/j.electacta.2009.05.013.
El Bouabi, Y., Farahi, A., Labjar, N., El Hajjaji, S., Bakasse, M., El Mhammedi, M.A., 2016. Square wave voltammetric determination of paracetamol at chitosan modified carbon

paste electrode: application in natural water samples, commercial tablets and human urines. Mater. Sci. Eng. C. 58, 70–77. https://doi.org/10.1016/j.msec.2015.08.014.
Ficek, M., Bogdanowicz, R., Ryl, J., 2015. Nanocrystalline CVD Diamond coatings on fused silica optical fibres: optical properties study. Acta Phys. Pol. A. 127, 868–873. https://doi.org/10.12693/APhysPolA.127.868.
Filanovsky, B., Markovsky, B., Bourenko, T., Perkas, N., Persky, R., Gedanken, A., Aurbach, D., 2007. Carbon electrodes modified with TiO2/metal nanoparticles and their application to the detection of trinitrotoluene. Adv. Funct. Mater. 17, 1487–1492. https://doi.org/10.1002/adfm.200600714.
Furton, K.G., Caraballo, N.I., Cerreta, M.M., Holness, H.K., 2015. Advances in the use of odour as forensic evidence through optimizing and standardizing instruments and canines. Philos. Trans. R. Soc. B Biol. Sci. 370. https://doi.org/10.1098/rstb.2014.0262.
Gao, Y.S., Xu, J.K., Lu, L.M., Wu, L.P., Zhang, K.X., Nie, T., Zhu, X.F., Wu, Y., 2014. Overoxidized polypyrrole/graphene nanocomposite with good electrochemical performance as novel electrode material for the detection of adenine and guanine. Biosens. Bioelectron. 62, 261–267. https://doi.org/10.1016/j.bios.2014.06.044.
Gaurav, A.K., Malik, P.K.Rai, 2009. Development of a new SPME-HPLC-UV method for the analysis of nitro explosives on reverse phase amide column and application to analysis of aqueous samples. J. Hazard. Mater. 172, 1652–1658. https://doi.org/10.1016/j.jhazmat.2009.08.039.
Goh, M.S., Pumera, M., 2011. Graphene-based electrochemical sensor for detection of 2,4,6- trinitrotoluene (TNT) in seawater: the comparison of single-, few-, and multilayer graphene nanoribbons and graphite microparticles. Anal. Bioanal. Chem. 399, 127–131. https://doi.org/10.1007/s00216-010-4338-8.
Grechishkin, V.S., Sinyavskii, N.Y., 2008. New technologies: nuclear quadrupole resonance as an explosive and narcotic detection technique. Uspekhi Fiz. Nauk. 167, 413. https://doi.org/10.3367/ufnr.0167.199704d.0413.
Guo, S., Wen, D., Zhai, Y., Dong, S., Wang, E., 2010. Platinum nanoparticle ensemble-on-electrode material for electrochemical rapid synthesis, and used as new graphene hybrid nanosheet: one-pot, sensing. ACS Nano 4, 3959–3968.
Harvey, S.D., Clauss, T.R.W., 1996. Rapid on-line chromatographic determination of trace-level munitions in aqueous samples. J. Chromatogr. A 753, 81–89. https://doi.org/10.1016/S0021-9673(96)00524-9.
Hundal, L.S., Singh, J., Bier, E.L., Shea, P.J., Comfort, S.D., Powers, W.L., 1997. Removal of TNT and RDX from water and soil using iron metal. Environ. Pollut. 97, 55–64.
Jamil, A.K.M., Izake, E.L., Sivanesan, A., Fredericks, P.M., 2015. Rapid detection of TNT in aqueous media by selective label free surface enhanced Raman spectroscopy. Talanta 134, 732–738. https://doi.org/10.1016/j.talanta.2014.12.022.
Junqueira, R.C., De Araujo, W.R., Salles, M.O., Paix, T.R.L.C., 2013. Flow injection analysis of picric acid explosive using a copper electrode as electrochemical detector. Talanta 104, 162–168. https://doi.org/10.1016/j.talanta.2012.11.036.
Lee, M.R., Chang, S.C., Kao, T.S., Tang, C.P., 1934. Studies of limit of detection on 2,4,6-Trinitrotoluene (TNT) by mss spectrometry. J. Res. Bur. Stand. (1934) 93 (1988), 428–430. https://doi.org/10.1038/159159b0.
López-López, M., García-Ruiz, C., 2014. Infrared and Raman spectroscopy techniques applied to identification of explosives. TrAC - Trends Anal. Chem. 54, 36–44. https://doi.org/10.1016/j.trac.2013.10.011.
Mozjoukhine, G.V., 2000. The two-frequency nuclear quadrupole resonance for explosives detection. Appl. Magn. Reson. 18, 527–535. https://doi.org/10.1007/BF03162299.
Muhammad, A., Yusof, N.A., Hajian, R., Abdullah, J., 2016. Construction of an electrochemical sensor based on carbon nanotubes/gold nanoparticles for trace determination of amoxicillin in bovine milk. Sensors (Switzerland) 16, 1–13. https://doi.org/10.3390/s16010056.
Narang, U., Gauger, P.R., Ligler, F.S., 1997. A displacement flow immunosensor for explosive detection using microcapillaries. Anal. Chem. 69, 2779–2785. https://doi.org/10.1021/ac970153d.
O'Mahony, A.M., Wang, J., 2013a. Nanomaterial-based electrochemical detection of explosives: a review of recent developments. Anal. Methods 5, 4296–4309. https://doi.org/10.1039/c3ay40636a.
O'Mahony, A.M., Wang, J., 2013b. Nanomaterial-based electrochemical detection of explosives: a review of recent developments. Anal. Methods 5, 4296–4309. https://doi.org/10.1039/c3ay40636a.
Oehrle, S.A., 2003. Analysis of nitramine and nitroaromatic explosives by capillary electrophoresis. J. Chromatogr. A 745, 233–237. https://doi.org/10.1016/0021-9673(96)00388-3.
Pittman, T.L., Thomson, B., Miao, W., 2009. Ultrasensitive detection of TNT in soil, water, using enhanced electrogenerated chemiluminescence. Anal. Chim. Acta 632, 197–202. https://doi.org/10.1016/j.aca.2008.11.032.
Pon Saravanan, N., Venugopalan, S., Senthilkumar, N., Santhosh, P., Kavita, B., Gurumallesh Prabu, H., 2006. Voltammetric determination of nitroaromatic and nitramine explosives contamination in soil. Talanta 69, 656–662. https://doi.org/10.1016/j.talanta.2005.10.041.
Protection, U.S.E., Epa, A., Facilities, F., Office, R., 2017. Technical fact sheet- 2,4,6-trinitrotoluene (TNT), United States. Environ. Prot. Agency. EPA 505-Fhttps://doi.org/10.1089/jpm.2012.0112.
Rabbany, S.Y., Lane, W.J., Marganski, W.A., Kusterbeck, A.W., Ligler, F.S., 2000. Trace detection of explosives using a membrane-based displacement immunoassay. J. Immunol. Methods 246, 69–77.
Riskin, M., Tel-Vered, R., Lioubashevski, O., Willner, I., 2009. Ultrasensitive surface plasmon resonance detection of trinitrotoluene by a bis-aniline-cross-linked Au nanoparticles composite. J. Am. Chem. Soc. 131, 7368–7378. https://doi.org/10.1021/ja9001212.
Ro, K.S., Venugopal, A., Adrian, D.D., Constant, D., Qaisi, K., Valsaraj, K.T., Thibodeaux, L.J., Roy, D., 1996. Solubility of 2,4,6-trinitrotoluene (TNT) in water. J. Chem. Eng. Data 41, 758–761. https://doi.org/10.1021/je950322w.
Roddey, H., Development, C., 2011. New Carbon Nanotube Sensor Can Detect Tiny Traces of Explosives. pp. 9–10.
Ryl, J., Burczyk, L., Bogdanowicz, R., Sobaszek, M., Darowicki, K., 2016. Study on surface termination of boron-doped diamond electrodes under anodic polarization in H2SO4 by means of dynamic impedance technique. Carbon N. Y. 96, 1093–1105.
Sağlam, Ş., Üzer, A., Erçağ, E., Apak, R., 2018. Electrochemical determination of TNT, DNT, RDX, and HMX with gold nanoparticles/poly(carbazole-aniline) film-modified glassy carbon sensor electrodes imprinted for molecular recognition of nitroaromatics and nitramines. Anal. Chem. 90, 7364–7370. https://doi.org/10.1021/acs.analchem.8b00715.
Sankaran, K.J., Ficek, M., Kunuku, S., Panda, K., Yeh, C.J., Park, J.Y., Sawczak, M., Michałowski, P.P., Leou, K.C., Bogdanowicz, R., Lin, I.N., Haenen, K., 2018. Self-organized multi-layered graphene-boron-doped diamond hybrid nanowalls for high-performance electron emission devices. Nanoscale 10, 1345–1355. https://doi.org/10.1039/c7nr06774g.
Šarlauskas, J., 2010. Polynitrobenzenes containing alkoxy and alkylenedioxy groups: potential hems and precursors of new energetic materials. Cent. Eur. J. Energy Mater. 7, 313–324.
Schnorr, J.M., Van Der Zwaag, D., Walish, J.J., Weizmann, Y., Swager, T.M., 2013. Sensory arrays of covalently functionalized single-walled carbon nanotubes for explosive detection. Adv. Funct. Mater. 23, 5285–5291. https://doi.org/10.1002/adfm.201300131.
Sekhar, P.K., Brosha, E.L., Mukundan, R., Linker, K.L., Brusseau, C., Garzon, F.H., 2011. Trace detection and discrimination of explosives using electrochemical potentiometric gas sensors. J. Hazard. Mater. 190, 125–132. https://doi.org/10.1016/j.jhazmat.2011.03.007.
Shankaran, D.R., Gobi, K.V., Sakai, T., Matsumoto, K., Toko, K., Miura, N., Gobi, K.V., Matsumoto, K., Miura, N., Shankaran, D.R., 2005. Surface plasmon resonance immunosensor for highly sensitive detection of 2,4,6-trinitrotoluene. Biosens. Bioelectron. 20, 1750–1756. https://doi.org/10.1016/j.bios.2004.06.044.
Singh, S., 2007. Sensors — an effective approach for the detection of explosives. J. Hazard. Mater. 144, 15–28. https://doi.org/10.1016/j.jhazmat.2007.02.018.
Siuzdak, K., Ficek, M., Sobaszek, M., Ryl, J., Gnyba, M., Niedziałkowski, P., Malinowska, N., Karczewski, J., Bogdanowicz, R., 2017a. Boron-enhanced growth of micron-scale carbon-based nanowalls: a route toward high rates of electrochemical biosensing. ACS Appl. Mater. Interfaces 9, 12982–12992. https://doi.org/10.1021/acsami.6b16860.
Siuzdak, K., Ficek, M., Sobaszek, M., Ryl, J., Gnyba, M., Niedziałkowski, P., Malinowska, N., Karczewski, J., Bogdanowicz, R., 2017b. Boron-enhanced growth of micron-scale carbon-based nanowalls: a route toward high rates of electrochemical biosensing. ACS Appl. Mater. Interfaces 9, 12982–12992. https://doi.org/10.1021/acsami.6b16860.
Sobaszek, M., Siuzdak, K., Ryl, J., Sawczak, M., Gupta, S., Carrizosa, S.B., Ficek, M., Dec, B., Darowicki, K., Bogdanowicz, R., 2017. Diamond phase (sp3-C) rich boron-doped carbon nanowalls (sp2-C): physicochemical and electrochemical properties. J. Phys. Chem. C. 121, 20821–20833. https://doi.org/10.1021/acs.jpcc.7b06365.
Soomro, R.A., Akyuz, O.P., Akin, H., Ozturk, R., Ibupoto, Z.H., 2016. Highly sensitive shape dependent electro-catalysis of TNT molecules using Pd and Pd-Pt alloy based nanostructures. RSC Adv. 6, 44955–44962. https://doi.org/10.1039/c6ra05588e.
Spencer, E.Y., Wright, G.F., 1946. Preparation of picramide. Can. J. Res. 24, 204–207. https://doi.org/10.1038/1811509b0.
Spiker, J.K., Crawford, D.L.O.N.L., Crawford, R.L., 1992. Influence of 2,4,6-trinitrotoluene (TNT) concentration on the degradation of TNT in explosive-contaminated soils by the white rot fungus Phanerochaete chrysosporium. Appl. Environ. Microbiol. 58, 3199–3202.
Stahl, D.C., Tilotta, D.C., 2001. Screening method for nitroaromatic compounds in water based on solid-phase microextraction and infrared spectroscopy. Environ. Sci. Technol. 35, 3507–3512. https://doi.org/10.1021/es010550c.
Toh, H.S., Ambrosi, A., Pumera, M., 2013. Electrocatalytic effect of ZnO nanoparticles on reduction of nitroaromatic compounds. Catal. Sci. Technol. 3, 123–127. https://doi.org/10.1039/c2cy20253k.
Tu, R., Liu, B., Wang, Z., Gao, D., Wang, F., Fang, Q., Zhang, Z., 2008. Amine-capped ZnS-Mn2+ nanocrystals for fluorescence detection of trace TNT explosive. Anal. Chem. 80, 3458–3465. https://doi.org/10.1021/ac800060f.
Wang, J., 2007. Electrochemical sensing of explosives, counterterrorist detect. Tech. Explos. 91–107. https://doi.org/10.1016/B978-044452204-7/50023-7.
Wang, J., Hocevar, S.B., Ogorevc, B., 2004. Carbon nanotube-modified glassy carbon electrode for adsorptive stripping voltammetric detection of ultratrace levels of 2,4,6-trinitrotoluene. Electrochem. Commun. 6, 176–179. https://doi.org/10.1016/j.elecom.2003.11.010.
Wang, P., Liu, Z.G., Chen, X., Meng, F.L., Liu, J.H., Huang, X.J., 2013. UV irradiation synthesis of an Au-graphene nanocomposite with enhanced electrochemical sensing properties. J. Mater. Chem. A 1, 9189–9195. https://doi.org/10.1039/c3ta11155e.
Wu, L., Almirall, J.R., Furton, K.G., 1999. An improved interface for coupling solid-phase microextraction (SPME) to high performance liquid chromatography (HPLC) applied to the analysis of explosives. HRC J. High Resolut. Chromatogr. 22, 279–282 doi:10.1002/(SICI)1521-4168(19990501)22:5 < 279::AID-JHRC279 > 3.0.CO;2-S.
Yew, Y.T., Ambrosi, A., Pumera, M., 2016. Nitroaromatic explosives detection using electrochemically exfoliated graphene. Sci. Rep. 6, 1–11. https://doi.org/10.1038/srep33276.
Yu, H.A., DeTata, D.A., Lewis, S.W., Silvester, D.S., 2017. Recent developments in the electrochemical detection of explosives: towards field-deployable devices for forensic science. TrAC - Trends Anal. Chem. 97, 374–384. https://doi.org/10.1016/j.trac.2017.10.007.
Yu, K., Bo, Z., Lu, G., Mao, S., Cui, S., Zhu, Y., Chen, X., Ruoff, R.S., Chen, J., 2011.

Growth of carbon nanowalls at atmospheric pressure for one-step gas sensor fabrication. Nanoscale Res. Lett. 6, 1–9. https://doi.org/10.1186/1556-276X-6-202.
Zeichner, A., Bronshtein, A., Altstein, M., Almog, J., Glattstein, B., Tamiri, T., 2002. Immunochemical approaches for purification and detection of TNT traces by antibodies entrapped in a sol – gel matrix. Anal. Chem. 73, 2461–2467. https://doi.org/10.1021/ac001376y.
Zhang, Y., Xu, M., Bunes, B.R., Wu, N., Gross, D.E., Moore, J.S., Zang, L., 2015a. Oligomer-coated carbon nanotube chemiresistive sensors for selective detection of nitroaromatic explosives. ACS Appl. Mater. Interfaces 7, 7471–7475. https://doi.org/10.1021/acsami.5b01532.
Zhang, H.X., Hu, J.S., Yan, C.J., Jiang, L., Wan, L.J., 2006a. Functionalized carbon nanotubes as sensitive materials for electrochemical detection of ultra-trace 2,4,6-trinitrotoluene. Phys. Chem. Chem. Phys. 8, 3567–3572. https://doi.org/10.1039/b604587c.
Zhang, R., Zhang, C., Zheng, F., Li, X., Sun, C., 2018a. Nitrogen and sulfur co-doped graphene nanoribbons : a novel metal-free catalyst for high performance electrochemical detection of 2, 4, 6- trinitrotoluene (TNT). Carbon 126, 328–337. https://doi.org/10.1016/j.carbon.2017.10.042.
Zhang, R., Zhang, C., Zheng, F., Li, X., Sun, C.L., Chen, W., 2018b. Nitrogen and sulfur co-doped graphene nanoribbons: a novel metal-free catalyst for high performance electrochemical detection of 2, 4, 6-trinitrotoluene (TNT). Carbon N. Y. 126, 328–337. https://doi.org/10.1016/j.carbon.2017.10.042.
Zhang, H.X., Cao, A.M., Hu, J.S., Wan, L.J., Lee, S.T., 2006b. Electrochemical sensor for detecting ultratrace nitroaromatic compounds using mesoporous SiO2-modified electrode. Anal. Chem. 78, 1967–1971. https://doi.org/10.1021/ac051826s.
Zhang, R., Sun, C.L., Lu, Y.J., Chen, W., 2015b. Graphene nanoribbon-supported PtPd concave nanocubes for electrochemical detection of TNT with high sensitivity and selectivity. Anal. Chem. 87, 12262–12269. https://doi.org/10.1021/acs.analchem.5b03390.